Electronic supplementary Information (ESI)

M13 Bacteriophage-templated Gold Nanowires as Stretchable Electrodes in Perovskite Solar Cells

Jiye Han,[‡a,b] Jeong-Seok Nam,[‡b] Kyusun Kim,[b] Eun Jung Choi,[c] Jong-Min Lee,[c] Shigeo Maruyama,[d,e] Il Jeon,[*b,d] Jin-Woo Oh[*a,c]

[a]*Department of Nano Fusion Technology, Pusan National University, 2, Busandaehak-ro 63beon-gil, Geumjeong-gu, Busan 46241, Republic of Korea*

[b]*Department of Chemistry Education, Graduate School of Chemical Materials, Institute for Plastic Information and Energy Materials, Pusan National University, 63-2 Busandaehak-ro, Busan 46241, South Korea*

[c]*Bio-IT Fusion Technology Research Institute, Pusan National University, 63-2 Busandaehak-ro, Busan 46241, South Korea*

[d]*Department of Mechanical Engineering, School of Engineering, The University of Tokyo, Tokyo 113-8656, Japan*

[e]*Energy NanoEngineering Lab., National Institute of Advanced Industrial Science and Technology (AIST), Tsukuba 305-8564, Japan*

AUTHOR INFORMATION

***Corresponding Authors**

*il.jeon@spc.oxon.org; *ojw@pusan.ac.kr

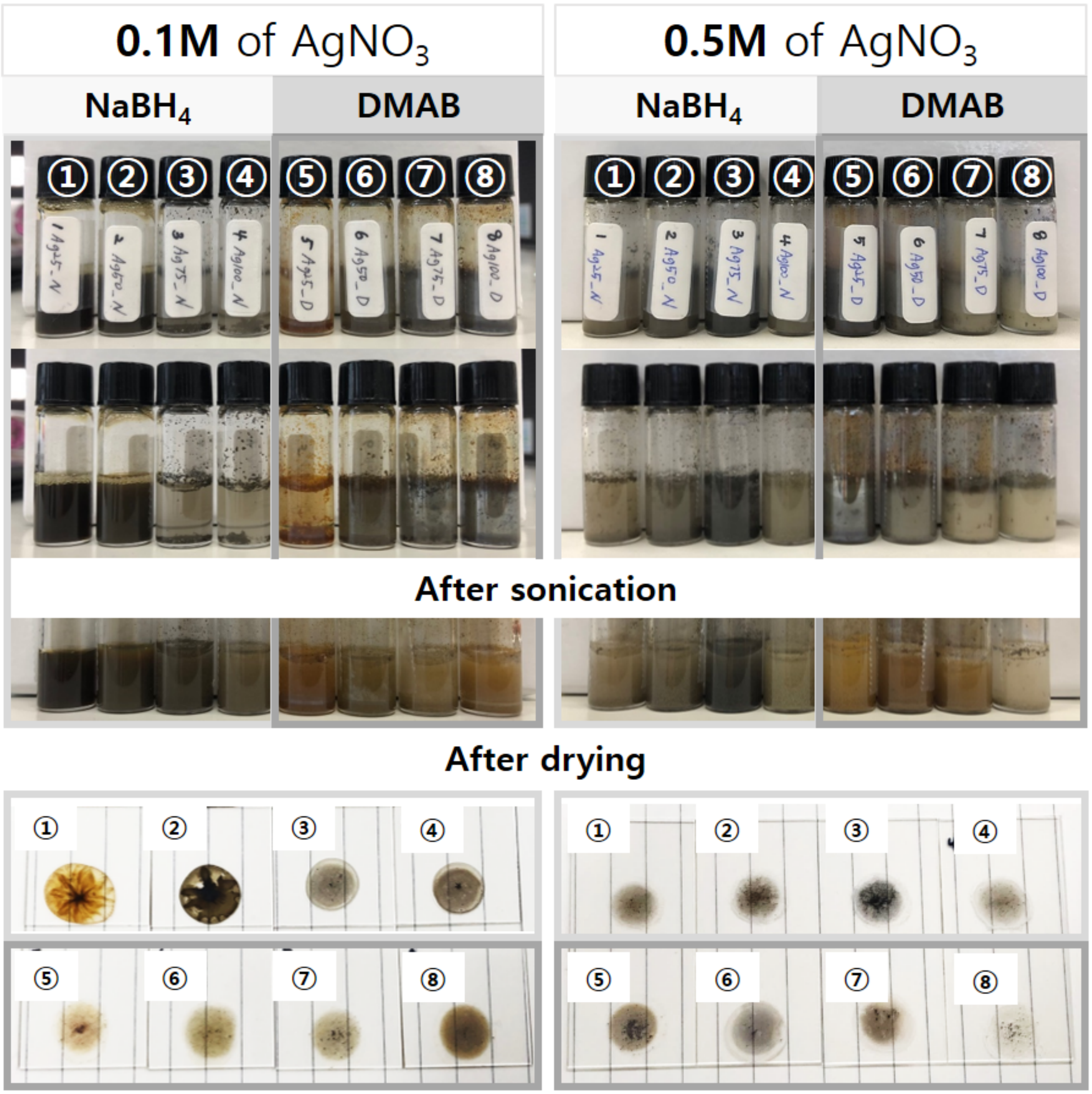

Fig. S1. Pictures showing the wild-type M13 bacteriophage with Ag particles under different concentrations and reducing agents. The resulting electrodes show low transparency.

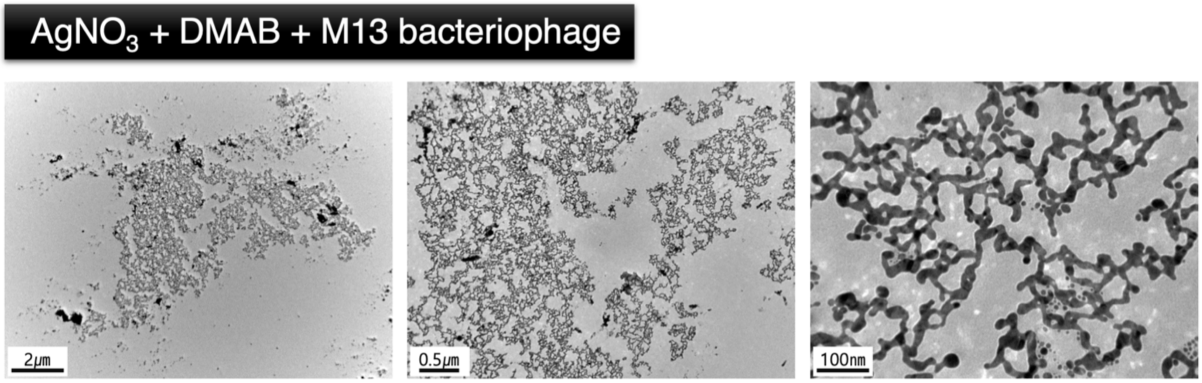

Fig. S2. Bio-TEM images of the mixture of $AgNO_3$, DMAB, and M13 bacteriophage.

DMAB

	0.1M $HAuCl_4$	0.5M $HAuCl_4$	1M $HAuCl_4$
Virus conc. (v/v %) 0	too high	too high	too high
Virus conc. (v/v %) 0.02	too high	374 Ω $sq.^{-1}$	437 Ω $sq.^{-1}$
Virus conc. (v/v %) 0.04	1270 Ω $sq.^{-1}$	300 Ω $sq.^{-1}$	469 Ω $sq.^{-1}$
Virus conc. (v/v %) 0.08	1420 Ω $sq.^{-1}$	682 Ω $sq.^{-1}$	592 Ω $sq.^{-1}$

$NaBH_4$

	0.1M $HAuCl_4$	0.5M $HAuCl_4$	1M $HAuCl_4$
Virus conc. (v/v %) 0	too high	too high	too high
Virus conc. (v/v %) 0.02	too high	77200 Ω $sq.^{-1}$	too high
Virus conc. (v/v %) 0.04	900000 Ω $sq.^{-1}$	30500 Ω $sq.^{-1}$	31700 Ω $sq.^{-1}$
Virus conc. (v/v %) 0.08	too high	87700 Ω $sq.^{-1}$	too high

Fig. S3. Sheet resistance values of virus-templated Au nanowire electrodes under different concentrations and reducing agents.

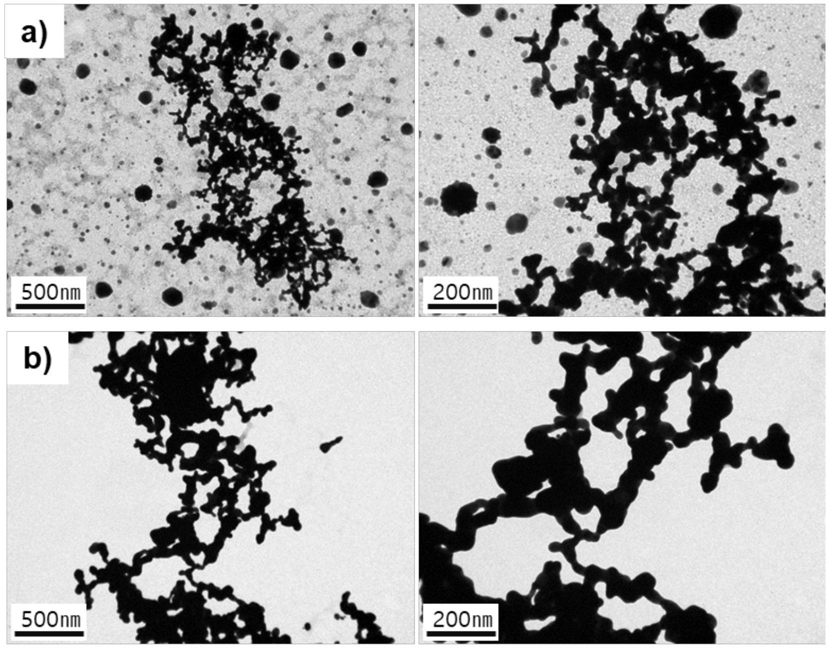

Fig. S4. Bio-TEM images showing change according to the type of reducing agent: a) DMAB and b) $NaBH_4$.

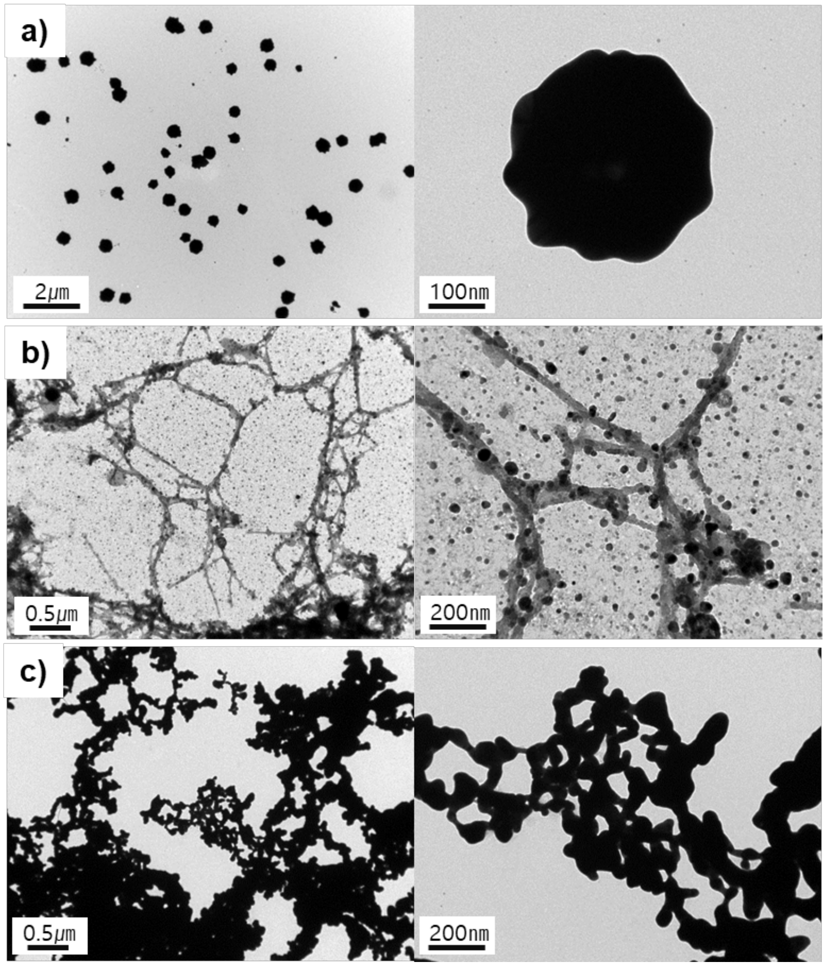

Fig. S5. Bio-TEM images of change with M13 virus conc.: a) 0 v/v %, b) 1 v/v %, and c) 5 v/v %.

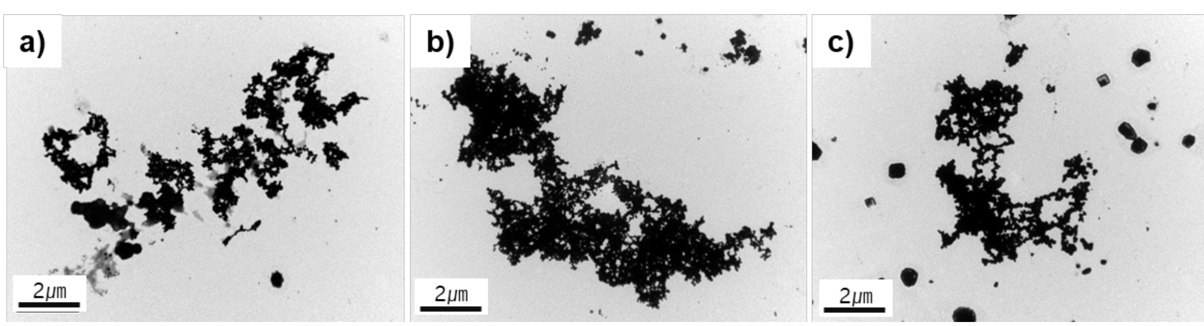

Fig. S6. Bio-TEM images of change with $HAuCl_4$ conc.: a) 0.2 mol L^{-1}, b) 0.5 mol L^{-1}, and c) 0.7 mol L^{-1}.

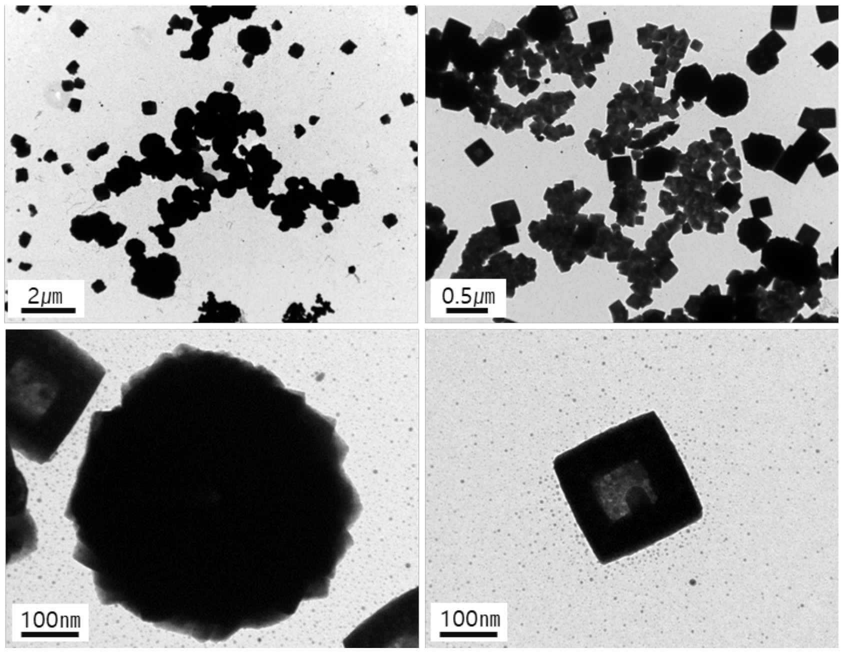

Fig. S7. Bio-TEM images of Au nanowire made using $NaBH_4$. It has impurities with different shapes, mostly cubic.

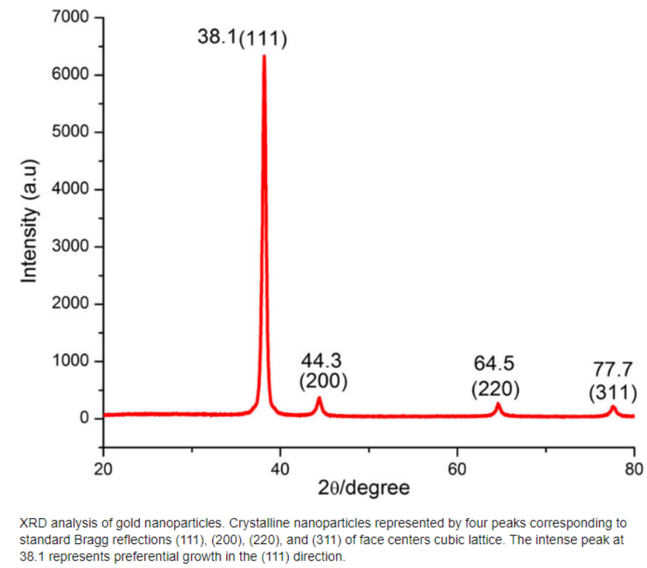

Fig. S8. Reported XRD spectrum of Au. Reproduced with permission.[S1] Copyright 2014, SpringerOpen.

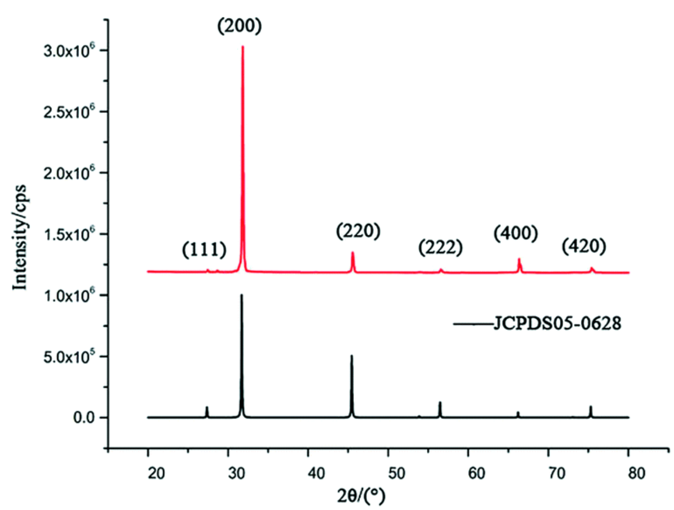

Fig. S9. Reported XRD spectrum of NaCl. Reproduced with permission.[S2] Copyright 2017, Royal Society of Chemistry.

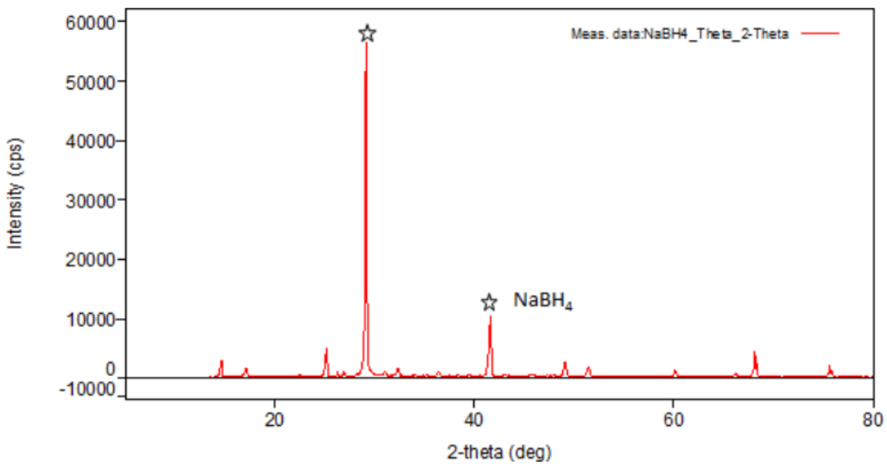

Fig. S10. Reported XRD spectrum of $NaBH_4$. Reproduced with permission.[S3] Copyright 2019, IOP Publishing.

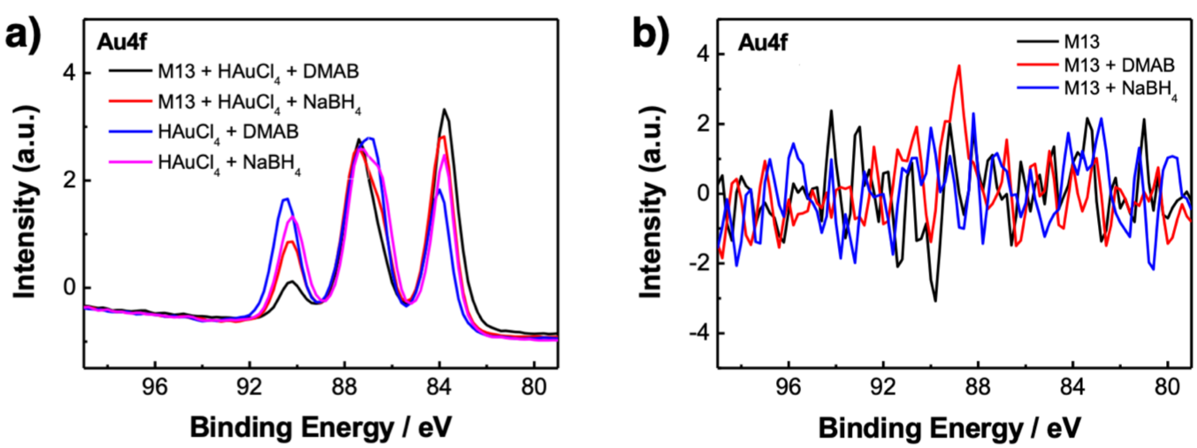

Fig. S11. XPS measurements of a) Au4f in M13 + $HAuCl_4$ + DMAB (black), M13 + $HAuCl_4$ + $NaBH_4$ (red), $HAuCl_4$ + DMAB (blue) and $HAuCl_4$ + $NaBH_4$ (pink), b) Au4f in M13 (black), M13+ DMAB (red) and M13 + $NaBH_4$ (blue).

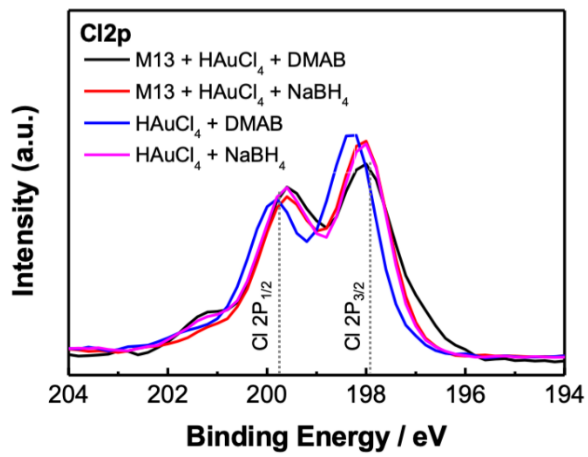

Fig. S12. XPS measurements of Cl2p in M13 + $HAuCl_4$ + DMAB (black), M13 + $HAuCl_4$ + $NaBH_4$ (red), $HAuCl_4$ + DMAB (blue), and $HAuCl_4$ + $NaBH_4$ (pink).

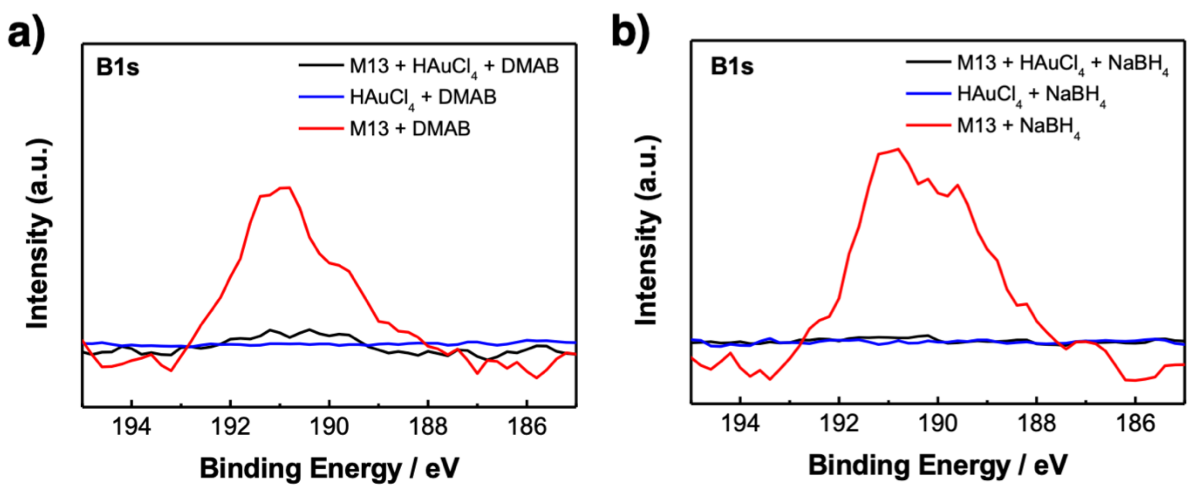

Fig. S13. XPS measurements of a) B1s in M13 + $HAuCl_4$ + DMAB (black), M13 + DMAB (blue), and M13 + DMAB (red), b) M13 + $HAuCl_4$ + $NaBH_4$ (black), $HAuCl_4$ + $NaBH_4$ (blue), and M13 + $NaBH_4$ (red).

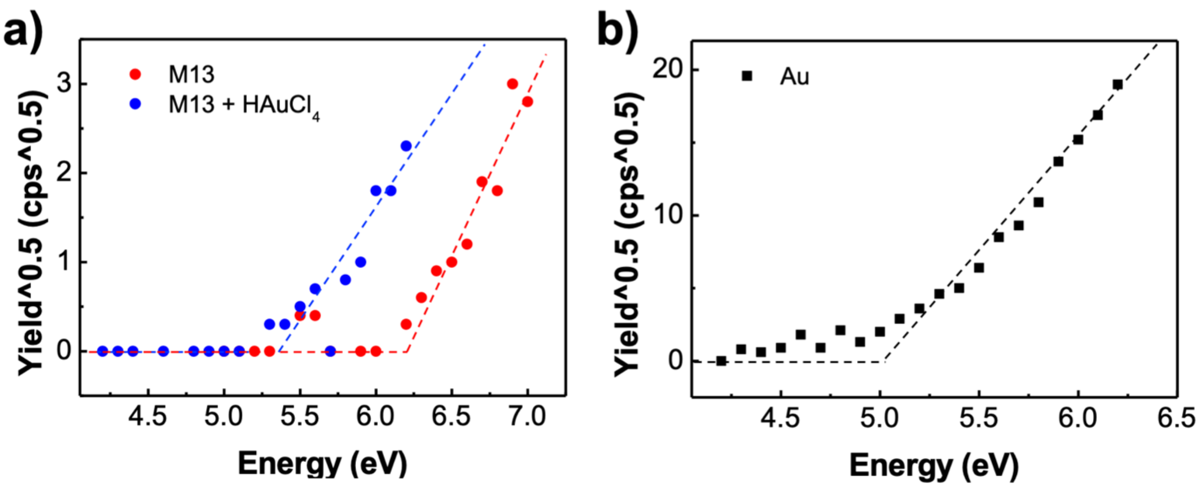

Fig. S14. PYS measurement of a) M13 bacteriophage only and DMAB-added virus-templated Au nanowires, and b) Au plate.

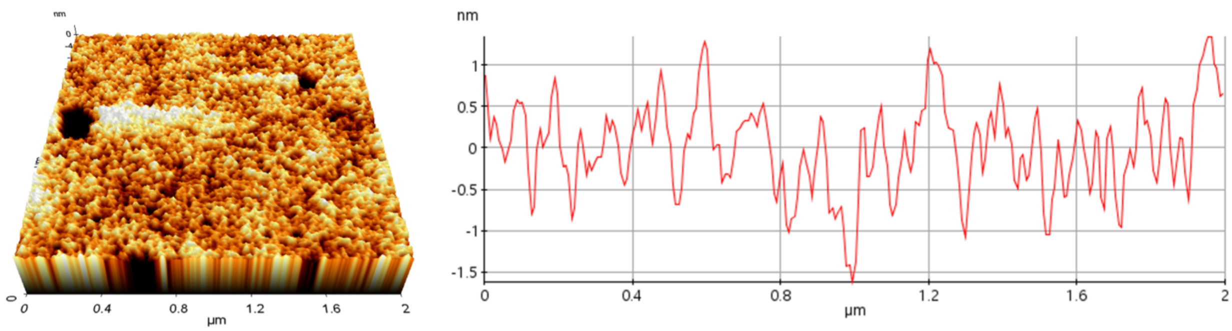

Fig. S15. AFM images ($2 \times 2\ \mu m^2$) of the PTAA-coated virus-templated Au nanowires on PDMS.

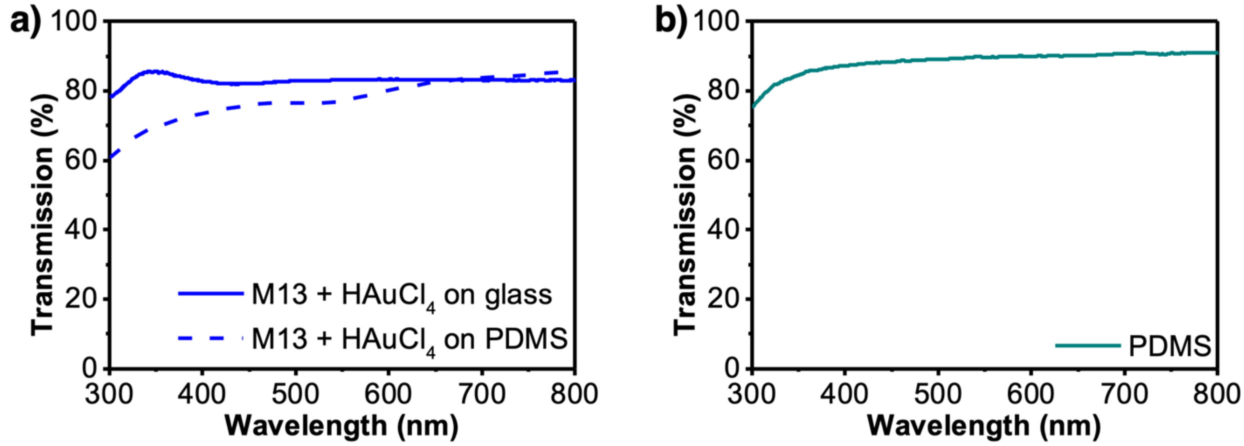

Fig. S16. Transmittance spectra of a) the virus-templated Au nanowire on glass and PDMS; and b) PDMS substrate only.

Table S1. Reported metal nanowire electrodes and their properties to date.

Year	Material Type	Deposition Technique	Transmittance (%)	Sheet resistance (Ω/sq)	Reference
2011	Au	N/A	83	49	S4
2011	Au	Lithography	83–95	30	S5
2013	Au	Self-assemble	80	70	S6
2013	Ag/CNT	Membrane filtering	82	4–24	S7
2015	Au	Dip-coating	70	50, > 40 MΩ	S8
2015	Ag/CNT/PEDOT:PSS	Membrane filtering	86	6.6	S9
2016	Au	Self-assemble	79	N/A	S10
2016	Au	Ink/nanoimprint	66	50	S11
2017	Ag	Spin-coating	~87	< 20	S12
2017	Au/Ag	Bar-coating	~80	10	S13
2018	Ag	Aerosol jet printing	72.3	57.68	S14
2019	Ag/ZnONP	Ultrasonic spray	85.5	2.48	S15
2019	Ag/LGO	Spin-coating	81.8	38.5	S16
2020	Ag/Graphene	Spin-coating	86.7	27	S17
2020	**Au/M13**	**Spin-coating**	**76.0**	**158.1**	**This Work**

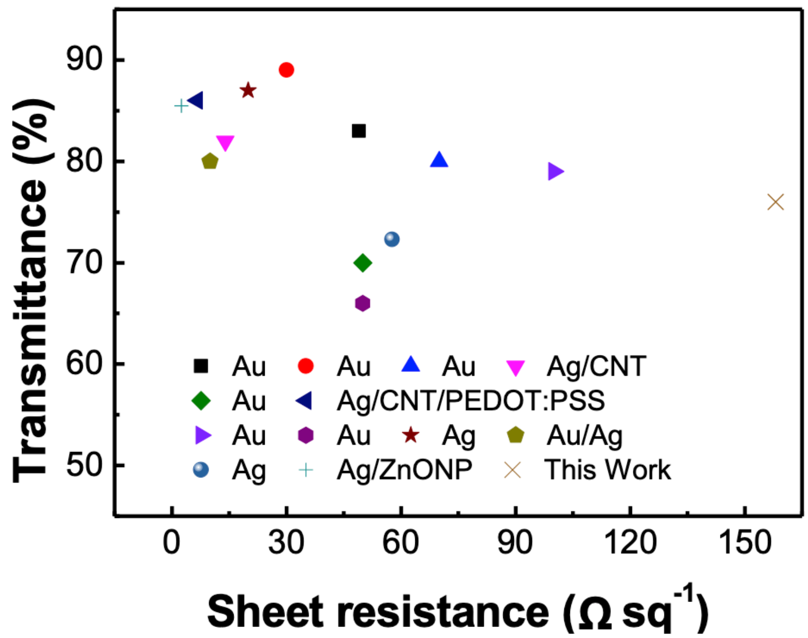

Fig. S17. Plot showing where the optical conductivity of our virus-templated Au nanowire electrode stands among the reported metal nanowire electrodes.

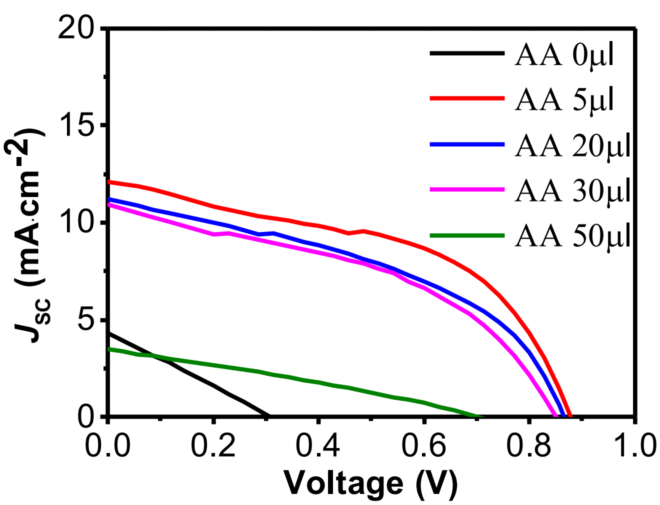

Fig. S18. *J*–*V* curves of the M13 Au nanowire-based PSCs made under different AA amounts for the optimisation.

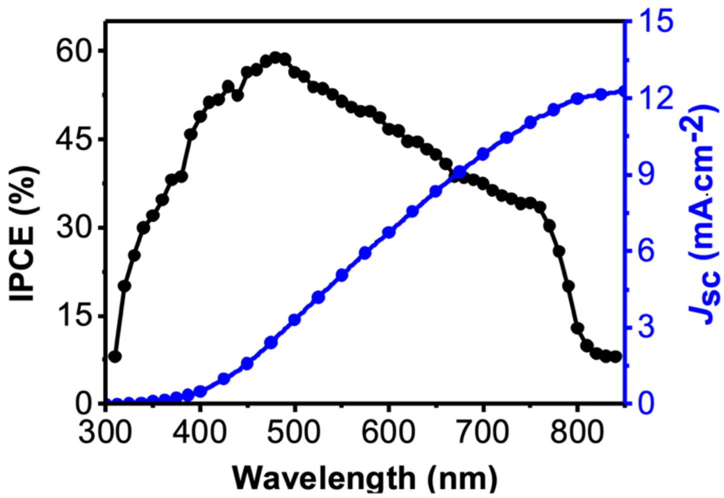

Fig. S19. Incident photon-to-electron conversion efficiency (IPCE) and integrated J_{SC} of the virus-templated Au nanowire-based PSCs.

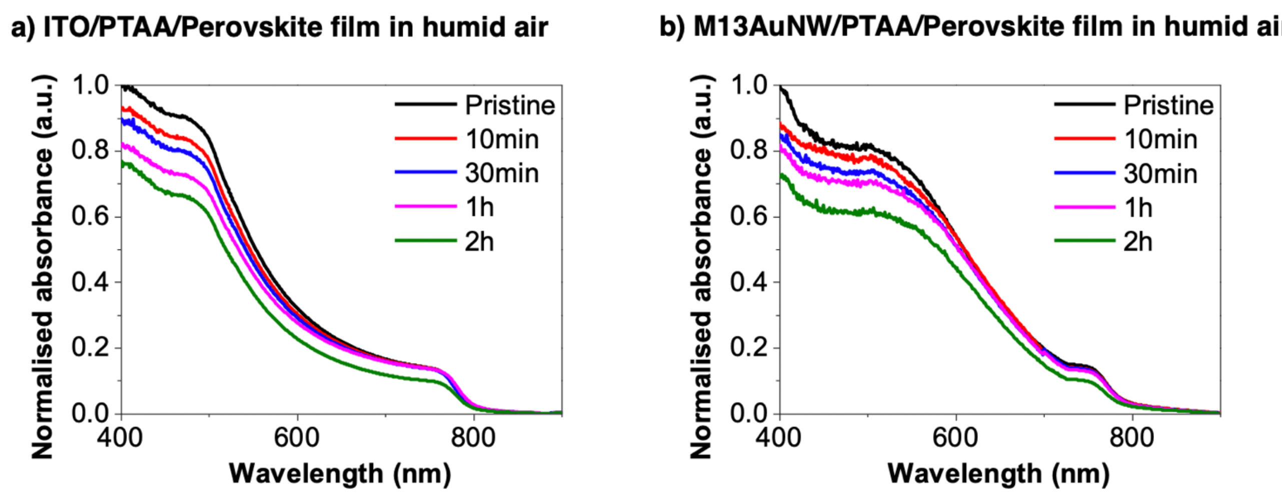

Fig. S20. Time-evolution of UV-vis absorption spectra of perovskite films on a) ITO and b) M13 virus-templated Au nanowires (M13AuNW) in humid conditions (RH ~60%).

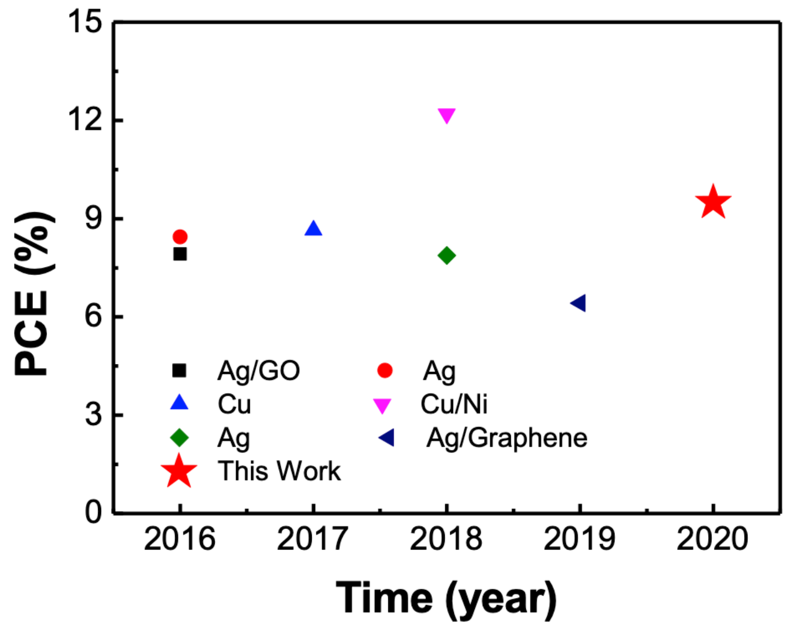

Fig. S21. PCEs of the reported metal nanowire transparent electrode-based PSCs.

Supplementary Reference

S1) S. Krishnamurthy, A. Esterle, N. C. Sharma and S. V. Sahi, *Nanoscale Res. Lett.*, 2014, **9**, 627.

S2) Y. Qin, D. Yu and J. Zhou, *CrystEngComm*, 2017, **19**, 5356–5360.

S3) D. Rohendi, N. Syarif and E. K. Wati, *IOP Conf. Ser. Earth Environ. Sci.*, 2019, **248**, 012008.

S4) P. E. Lyons, S. De, J. Elias, M. Schamel, L. Philippe, A. T. Bellew, J. J. Boland and J. N. Coleman, *J. Phys. Chem. Lett.*, 2011, **2**, 3058–3062.

S5) M. C. Rosamond, A. J. Gallant, J. J. Atherton, M. C. Petty, O. Kolosov and D. A. Zeze, in *2011 11th IEEE International Conference on Nanotechnology*, IEEE, 2011, pp. 604–607.

S6) A. Morag, V. Ezersky, N. Froumin, D. Mogiliansky and R. Jelinek, *Chem. Commun.*, 2013, **49**, 8552.

S7) A. J. Stapleton, R. A. Afre, A. V. Ellis, J. G. Shapter, G. G. Andersson, J. S. Quinton and D. A. Lewis, *Sci. Technol. Adv. Mater.*, 2013, **14**, 035004.

S8) J. H. M. Maurer, L. González-García, B. Reiser, I. Kanelidis and T. Kraus, *ACS Appl. Mater. Interfaces*, 2015, **7**, 7838–7842.

S9) A. J. Stapleton, S. D. Yambem, A. H. Johns, R. A. Afre, A. V. Ellis, J. G. Shapter, G. G. Andersson, J. S. Quinton, P. L. Burn, P. Meredith and D. A. Lewis, *Sci. Technol. Adv. Mater.*, 2015, **16**, 025002.

S10) S. Gong, Y. Zhao, Q. Shi, Y. Wang, L. W. Yap and W. Cheng, *Electroanalysis*, 2016, **28**, 1298–1304.

S11) J. H. M. Maurer, L. González-García, B. Reiser, I. Kanelidis and T. Kraus, *Nano Lett.*, 2016, **16**, 2921–2925.

S12) P. Kou, L. Yang, C. Chang and S. He, *Sci. Rep.*, 2017, **7**, 42052.

S13) S. Kim, B. Kim, I. Im, D. Kim, H. Lee, J. Nam, H. Kyoon Chung, H.-J. Lee and S. Min Cho, *Nanotechnology*, 2017, **28**, 345201.

S14) L. Tu, S. Yuan, H. Zhang, P. Wang, X. Cui, J. Wang, Y.-Q. Zhan and L.-R. Zheng, *J. Appl. Phys.*, 2018, **123**, 174905.

S15) D. Kumar, V. Stoichkov, E. Brousseau, G. C. Smith and J. Kettle, *Nanoscale*, 2019, **11**, 5760–5769.

S16) H. Chen, M. Li, X. Wen, Y. Yang, D. He, W. Choy and H. Lu, *Nanomaterials*, 2019, **9**, 193.

S17) H. Li, Y. Liu, A. Su, J. Wang and Y. Duan, *Sci. Rep.*, 2019, **9**, 17998.